SCIENTIFIC REPORTS

OPEN

SUBJECT AREAS:

ATOMIC AND MOLECULAR INTERACTIONS WITH PHOTONS

ATTOSECOND SCIENCE

ATOMIC AND MOLECULAR PHYSICS

ELECTRONIC STRUCTURE OF ATOMS AND MOLECULES

Received
6 June 2013

Accepted
21 August 2013

Published
17 September 2013

Correspondence and requests for materials should be addressed to J.B. (jens.biegert@icfo.eu)

Ionization with low-frequency fields in the tunneling regime

J. Dura[1], N. Camus[2], A. Thai[1], A. Britz[1], M. Hemmer[1], M. Baudisch[1], A. Senftleben[2], C. D. Schröter[2], J. Ullrich[2,3], R. Moshammer[2] & J. Biegert[1,4]

[1]ICFO-Institut de Ciences Fotoniques, 08860 Castelldefels (Barcelona), Spain, [2]Max-Planck-Institut für Kernphysik, Saupfercheckweg 1, 69117 Heidelberg, Germany, [3]Physikalisch-Technische Bundesanstalt, D-38116 Braunschweig, Germany, [4]ICREA – Institució Catalana de Recerca i Estudis Avançats, 08010 Barcelona, Spain.

Strong-field ionisation surprises with richness beyond current understanding despite decade long investigations. Ionisation with mid-IR light has promptly revealed unexpected kinetic energy structures that seem related to unanticipated quantum trajectories of the electrons. We measure first 3D momentum distributions in the deep tunneling regime ($\gamma = 0.3$) and observe surprising new electron dynamics of near-zero momentum electrons and extremely low momentum structures, below the eV, despite very high quiver energies of 95 eV. Such level of high-precision measurements at only 1 meV above the threshold, despite 5 orders higher ponderomotive energies, has now become possible with a specifically developed ultrafast mid-IR light source in combination with a reaction microscope, thereby permitting a new level of investigations into mid-IR recollision physics.

Ionization of an atom or molecule presents surprising richness beyond our current understanding: strong-field ionization with low-frequency fields recently revealed unexpected kinetic energy structures[1,2]. A solid grasp on electron dynamics is however pre-requisite for attosecond-resolution recollision imaging[3], orbital tomography[4], for coherent sources of keV light[5], or to produce zeptosecond-duration x-rays[6].

Full scrutiny of strong field processes requires a light source reaching relevant field strengths with repeatable electric field waveforms, and 3D momentum detection. Mid-IR probing removes ambiguities between tunneling and multi-photon processes, but unfavorable scaling of cross-sections, and lack of mid-IR ultrafast technology, has largely prevented this approach. We now enable such measurements with a specifically designed mid-IR light source[7] (see Methods), which fulfills all requirements and is perfectly matched to a reaction microscope thereby permitting rapid and high-precision data acquisition. We show here the power of our method by applying it to the recent unexpected low-energy structures (LES).

The LES was first observed by Blaga *et al.*[1] at several eV, when ionizing argon and xenon atoms (also molecular hydrogen and nitrogen) with short pulses at long wavelengths. Quan *et al.*[2] showed similar results shortly thereafter for xenon. Recently, Wu *et al.*[8] observed even slower electrons (just below 1 eV), for similar conditions in krypton and xenon, termed very low energy structure (VLES). The VLES seems to persist for 800 nm in neon even though it is hard to identify. It is difficult to disentangle the origin of the various findings without momentum distribution measurements for LES or VLES; moreover, experimental conditions, varied across these investigations. Without momentum information, the appearance of VLES, and for LES, was attributed to long-range Coulomb effects.

On the theory side, models based on the strong-field approximation (SFA)[1] were unable to predict the LES. Comparison of SFA, which neglects the ion's Coulomb field, with ab-initio calculations supported the assumption of the ion's Coulomb field as responsible for the modification of electron trajectories[1,9–17]. Direct tunneling close to a local field maximum, even though resulting in low-energy photoelectrons (until $2U_p$; ponderomotive energy $U_p = E^2/4\omega^2$; E is the peak electric field amplitude and ω the laser frequency in atomic units), is therefore seen as an unlikely cause of the LES. The location of the LES, at energies far below $2U_p$, would exclude rescattering ($2U_p$ to $10U_p$) as underlying mechanism, while its disappearance with circularly polarized light[1] would contradict this notion. Faisal pointed out[18] that forward scattering from the successive half-cycle, could be another competing channel, which should be considered. Several theoretical investigations quickly confirmed the strong contribution from forward-scattering[9,10,12,14,16] and, therefore, identified the LES as resulting from soft recollisions modified by the interaction of the outgoing electron with the ion's Coulomb field[9,10]. Very recent calculations[17]

also attribute the origin of the VLES (or second order LES, as quoted in[17]) to soft rescattering, with the Coulomb force acting only on the radial component of the electron's motion.

In a recent publication Liu *et al.*[19] report opposing experimental findings: they observe low yield of low kinetic energy electrons from strong-field ionization of krypton and xenon atoms using 1320 nm light and at similar pulse peak intensity as in the previously cited experimental papers. The authors attribute their contradicting observations to population trapping in high-lying (Rydberg) states as suppression mechanism. In fact, the possibility of an atom resisting ionization by a strong laser field has been pointed out early on by Fedorov[20] and others[21] in the multi-photon picture and in the tunneling regime[22,23]; this mechanism was termed as frustrated tunnel ionization[24]. We note that, aside from the contradicting measurements, the existence of such local ionization suppression is under debate and some authors question the mechanism altogether[25]. Thus, one is faced with a situation that there are surprising new findings on low-energy photoelectron spectra and angular distributions in the mid-IR laser wavelength regime that were neither anticipated by theory nor are they consistently explained.

Thus, the goal of our investigation was providing high-resolution 3D electron momentum data for strong-field ionization by low-frequency laser fields for argon atoms and oxygen molecules, thereby creating the basis for further experimental investigations and theoretical studies. Ar and O_2, resemble the most thoroughly scrutinized atomic and simple molecular systems, therefore providing a benchmark for future theoretical and experimental discussions. We specifically elect O_2, and not argon's molecular partner N_2, since nitrogen is known to exhibit similar response to argon upon ionization, while O_2 exhibits a very different response due to its different electronic structure. Our measurements have become possible in the non-perturbative, non-relativistic tunneling regime (Keldysh adiabaticity parameter[26] $\gamma = \sqrt{I_p/2U_p} = 0.3 \ll 1$, U_p = 95 eV, z = 237 and z_1 = 11; $a_0 = eE/m\omega = 0.027 \ll 1$) due to the development of a unique high-repetition rate (160 kHz) source of intense and carrier-to-envelope phase (CEP) stable, few-cycle pulses in the mid-IR[27] (6 cycle duration, 3100 nm (0.4 eV or 0.015 a.u), 16 μJ), which is prerequisite for 3D momentum imaging with a reaction microscope (REMI); details on the source and detector can be found in Methods.

Results

Our kinematically complete measurement permits an unprecedented view at low-frequency photoionization enabling identification of its underlying contributions. We find striking new features in Fig. 1(a); $P_{parallel}$ is the momentum parallel to the laser's electric field direction (in our case along the z-axis; i.e. $P_{parallel} = P_z$) and $P_{transverse}$ ($= \sqrt{P_x^2 + P_y^2}$) is the momentum normal to $P_{parallel}$. Similar features are observed for oxygen in Suppl. Fig. 1. We find, for Ar ($P_{parallel} <$ 0.4 a.u. (2.18 eV), and $P_{transverse} <$ 0.5 a.u. (3.4 eV) an extremely narrow contribution ("zero-peak") of zero, or near-zero momentum electrons (I) and, emanating from there, a "v-like" pattern (II) which

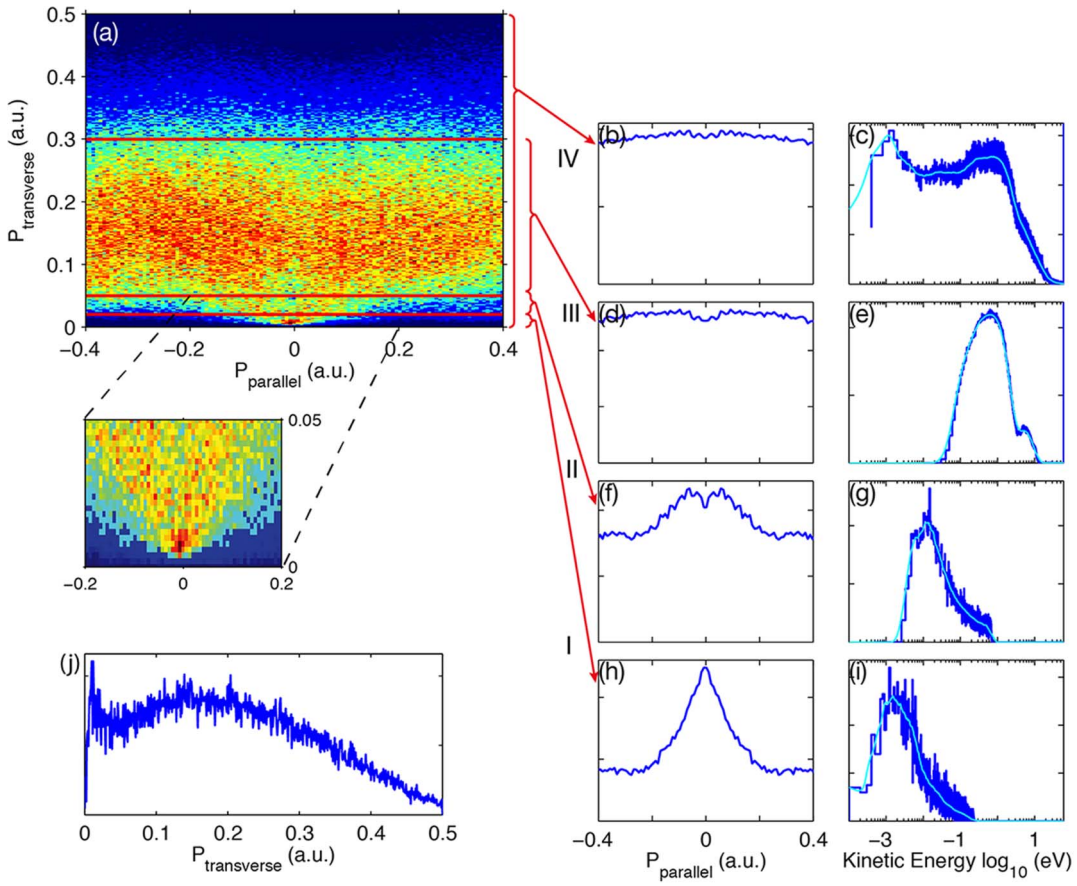

Figure 1 | Electron momentum distributions and correlated total kinetic energy for Ar. Graph (b) shows the parallel electron momentum and (c) the angle integrated electron kinetic energy for the complete distribution (a). The following graphs highlight contributions from the various areas (I, II and III) within the momentum map (a) to parallel electron momenta (b,d,f,h) and angle integrated kinetic energy (c,e,g,i). Zero-, or near-zero-momentum electrons (I) contribute in the meV to the kinetic energy spectrum (i), to a peak at zero parallel electron momentum (h) and to a peak at zero-, or near-zero-transverse momentum (j). A "v"-like structure (II) is visible at slightly larger transverse momenta, corresponding to a narrow double-hump structure in the parallel electron momentum spectrum (f) which is different from the broad momentum distribution (e), associated with LES, which results in a broad hump-like structure (d).

widens and merges with the broad distribution (III) at larger transverse momenta. We analyze the kinetic energy spectrum and parallel momentum distribution for the individual areas (I, II, III) and identify the broad contribution of area III (0.06 a.u. to 0.3 a.u transverse momentum) as LES according to the kinetic energy spectrum (Fig. 1(e)). Associated with this area is a broad double hump structure in parallel momentum (Fig. 1(d)) that is significantly narrower (Fig. 1(f)) for area II. We note that multiple recollisions leading to interference between the outgoing electron waves and the rescattered ones have been identified as leading to sharp "SPIDER-like" nodal patterns[28,29]. They were however observed at momenta corresponding to LES, rather than VLES, as in this experiment. The kinetic energy spectrum (Fig. 1(g)) permits identifying the "v-like" distribution as the VLES. Most striking is the convergence of the "v-like" structure into an extremely narrow contribution extending towards zero momentum (I) despite quiver energy of 95 eV. The offset of the "zero-peak" from zero transverse momentum is within our measurement resolution of $|(0.008 \pm 0.026)|$ a.u. in the transverse and (0 ± 0.012) a.u. in the parallel direction.

Discussion

Our measurement allows, for the first time, disentangling parallel momentum contributions as originating from VLES and LES. The persistence of VLES at shorter wavelength[8] and the absence of LES would indicate that the previously found double-hump structures[30,31] are reminiscent of VLES. Areas (I) and (II) show never-observed features which we find as being of very general nature for the different target species investigated and varying in their relative contributions. Measurements in oxygen, Suppl. Fig. 1, show less slow electrons, but the zero kinetic-energy feature is clearly visible. Our observation is consistent with previous findings of Rudenko *et al.*[30] and Liu *et al.*[31] who have observed a zero momentum peak in the parallel ion momentum of argon and oxygen respectively but not for other molecules and noble gases.

Both features (Fig. 1(f,g and (h,i))) disappear when introducing 15% ellipticity (see Fig. 2). Figure 2 shows measurements of the 3D integrated photoelectron kinetic-energy spectrum for linear and elliptically polarized light. We find, analogously to Ref. 1, the LES peaks at higher kinetic energy for elliptically polarized light and our newly observed feature at 1.3 meV is not discernible any more. Note that the peak at 1.3 meV is within our experimental resolution of 11 meV. Persistence of the "zero-peak" across various species, and its disappearance when ionizing with circularly polarized light suggests involvement of electron rescattering[9–17]. What could the cause for the low momentum be? Trapping of population in high lying, or Rydberg, states[13,22,23] could, ultimately, result in electrons[21] with very small momenta[32]. Figure 3 indeed evidences strong interaction with the ion's field, which could be responsible for electron trapping after tunneling[22,24]: deviation from a Gaussian-like distribution, in favor of a cusp-like distribution, in one of the perpendicular components of the electron momenta, we plot P_x, is the unambiguous signature of the Coulomb field[33]. We find the lowest energy electrons show the strongest deviation (Fig. 1(h)); analog findings are shown in Suppl. Fig. 2 for O_2 molecules. The hypothesis of involvement of high-lying states, ultimately leading to low-momentum electrons, is also supported by elliptically polarized light reducing population in high-lying states[24,34]; this would explain the absence of low kinetic-energy electrons with elliptically polarized light.

Our method enables a new level of high precision strong field measurements and sheds new light on recollision dynamics with striking new findings. We observe unseen "v-like" patterns in the electron's momentum distribution and exceptionally slow electrons at near-zero momentum. These measurements reveal a much more intricate and less trivial behavior of atoms and simple molecules under strong mid-IR fields than previously observed or expected. The persistence of these findings is independent on electronic structure and hints at quantum interference, due to the strong external field with the ion's Coulomb field, and the importance of transient intermediate states. We are currently working in this direction to further corroborate our findings. Our results are important for realizing the enticing possibilities of mid-IR rescattering physics, which require a firm grasp on the underlying electron dynamics.

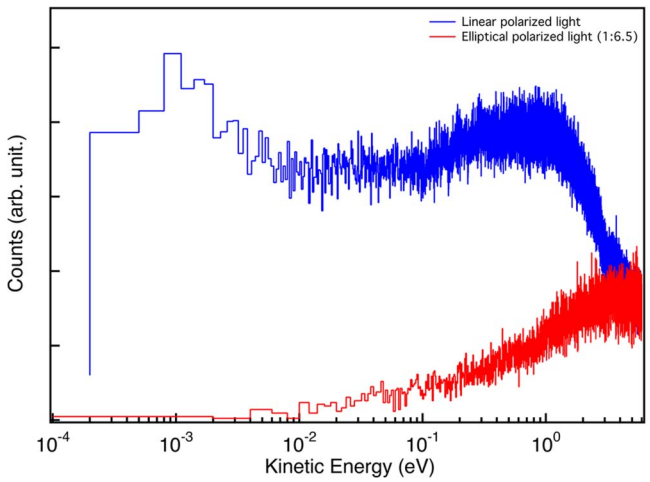

Figure 2 | Photoelectron kinetic energy for Ar. Total kinetic energy spectrum for the photoelectrons, integrated over 4π steradian. Shown is the case for irradiation with linear polarization and 15% ellipticity; both for randomized CEP.

Methods

Mid-IR light source. The experiments were performed with our home-built mid-IR optical parametric chirped pulse amplifier (OPCPA)[35], which delivers linearly polarized, 60-fs (6-cycle) pulses at 3100 nm centre wavelength and 160 kHz pulse repetition rate. Pulse energies of up to 16 μJ are achieved after compression with a power stability of better than 0.3% rms and 0.8% peak-to-peak over 15 hours. The OPCPA is optically carrier-to-envelope phase (CEP) self-stabilized and routinely achieves 250 mrad stability over 30 min. We refer for a detailed description of our OPCPA light source to Refs. 27,35.

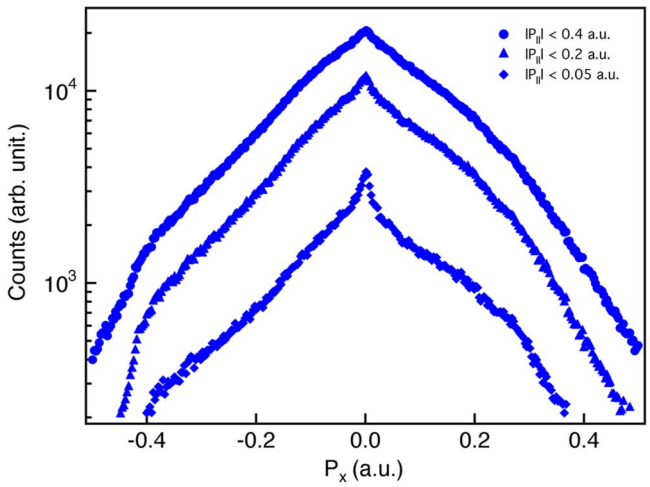

Figure 3 | Perpendicular component of electron momentum distributions for Ar. P_x component of the electron momentum, perpendicular to the laser polarization, for different integration ranges along the parallel momentum as indicated in the figure and highlighted by different symbols. The strong influence of the Coulomb potential manifests itself for the smallest longitudinal momentum cut in form of a strong cusp-like feature (diamonds).

Reaction microscope. High-pressure gas is supersonically expanded into vacuum and skimmed in two successive stages to deliver a cold and directed atomic beam into the target chamber of the REMI. We use a mass flow controller to ensure identical number density of $10^{11}/cm^3$ for all target species used in our experiments. The target momentum resolution is estimated as 0.03 a.u. in jet direction and 0.012 a.u. perpendicularly. Momentum accuracy is 0.025 a.u. transversally and 0.012 a.u. parallel to the laser field. 8 μJ-energy pulses are focused with an on-axis, gold-coated, 1.2 f-number paraboloid into the gas jet, forming a 6 μm-width focal region. Upon ionization, electrons and ions are separated by a weak electric field (1.5 V/cm) and guided towards opposing micro channel plate (MCP) detectors equipped with delay line readout. Helmholtz coils generate a homogenous magnetic field (460 μT) to ensure near 4π collection efficiency for the fragments of interest. The jet is extracted separately to ensure a backing pressure of the REMI of 6×10^{-9} mbar (without jet 3×10^{-11} mbar). Time-of-flight (TOF) information is extracted from the MCP detectors, which are triggered from a fast photodiode (PD). The delay-line readout provides position information and the combination with TOF permits reconstructing 3D momentum vectors for ions and electrons in coincidence. We operate the gas jet at a density low enough to ensure an average count rate of 0.03 per pulse in order to minimize false coincidences. Data was collected over duration of 21 hours at the full repetition rate of the laser system at 160 kHz and in coincidence. The data set for argon contains 9×10^6 coincidence events.

1. Blaga, C. *et al*. Strong-field photoionization revisited. *Nat. Phys.* **5**, 335–338 (2008).
2. Quan, W. *et al*. Classical aspects in above-threshold ionization with a midinfrared strong laser field. *Phys. Rev. Lett.* **103**, 093001 (2009).
3. Xu, J., Chen, Z., Le, A. & Lin, C. Self-imaging of molecules from diffraction spectra by laser-induced rescattering electrons. *Phys. Rev. A* **82**, 033403 (2010).
4. Itatani, J. *et al*. Tomographic imaging of molecular orbitals. *Nature* **432**, 867–871 (2004).
5. Chen, M. C. *et al*. Bright, coherent, ultrafast soft x-ray harmonics spanning the water window from a tabletop light source. *Phys. Rev. Lett.* **105**, 173901 (2010).
6. Popmintchev, T., Chen, M.-C., Arpin, P., Murnane, M. M. & Kapteyn, H. C. The attosecond nonlinear optics of bright coherent x-ray generation. *Nature Photonics* **4**, 822–832 (2010).
7. Biegert, J., Bates, P. & Chalus, O. New mid-infrared light sources. *IEEE J. Sel. Top. Quant. Elec.* **18**, 531–540 (2012).
8. Wu, C. *et al*. Characteristic spectrum of very low-energy photoelectron from above-threshold ionization in the tunneling regime. *Phys. Rev. Lett.* **109**, 043001 (2012).
9. Liu, C. & Hatsagortsyan, K. Origin of unexpected low energy structure in photoelectron spectra induced by mid- infrared strong laser fields. *Phys. Rev. Lett.* **105**, 113003 (2010).
10. Yan, T.-M., Popruzhenko, S. V., Vrakking, M. J. J. & Bauer, D. Low-energy structures in strong field ionization revealed by quantum orbits. *Phys. Rev. Lett.* **105**, 253002 (2010).
11. Huang, C., Liao, Q., Zhou, Y. & Lu, P. Role of coulomb focusing on the electron transverse momentum of above- threshold ionization. *Opt. Expr.* **18**, 14293–14300 (2010).
12. Kastner, A., Saalmann, U. & Rost, J. Electron-energy bunching in laser-driven soft recollisions. *Phys. Rev. Lett.* **108**, 033201 (2012).
13. Burenkov, I., Popov, A., Tikhonova, O. & Volkova, E. New feature of the interaction of atomic and molecular systems with intense ultrashort laser pulses. *Laser Phys. Lett.* **7**, 409–434 (2010).
14. Lemell, C. *et al*. Low-energy peak structure in strong-field ionization by midinfrared laser pulses: Two-dimensional focusing by the atomic potential. *Phys. Rev. A* **85**, 011403 (2012).
15. Telnov, D. & Chu, S.-I. Low-energy structure of above- threshold-ionization electron spectra: Role of the coulomb threshold effect. *Phys. Rev. A* **83**, 063406 (2011).
16. Liu, C. & Hatsagortsyan, K. Coulomb focusing in above-threshold ionization in elliptically polarized midinfrared strong laser fields. *Phys. Rev. A* **85**, 023413 (2012).
17. Lemell, C. *et al*. Classical-quantum correspondence in atomic ionization by midinfrared pulses: Multiple peak and interference structures. *Phys. Rev. A* **87**, 013421 (2013).
18. Faisal, F. Strong-field physics: Ionization surprise. *Nature Physics* **5**, 319–320 (2009).
19. Liu, H. *et al*. Low yield of near-zero-momentum electrons and partial atomic stabilization in strong-field tunneling ionization. *Phys. Rev. Lett.* **109**, 093001 (2012).
20. Fedorov, M. & Movsesian, A. Field-induced effects of narrowing of photoelectron-spectra and stabilization of rydberg atoms. *J. Phys. B-At. Mol. Opt. Phys.* **21**, L155–L158 (1988).
21. Ivanov, M. Trapping of population at Rrydberg states during strong-field multiphoton ionization. *Laser Phys.* **3**, 640–643 (1993).
22. Yudin, G. & Ivanov, M. Physics of correlated double ionization of atoms in intense laser fields: Quasistatic tunneling limit. *Phys. Rev. A* **63**, 033404 (2001).
23. Shvetsov-Shilovski, N. I., Goreslavski, S. P., Popruzhenko, S. V. & Becker, W. Capture into Rydberg states and momentum distributions of ionized electrons. *Laser Phys.* **19**, 1550–1558 (2009).
24. Nubbemeyer, T., Gorling, K., Saenz, A., Eichmann, U. & Sandner, W. Strong-field tunneling without ionization. *Phys. Rev. Lett.* **101**, 233001 (2008).
25. Gavrilenko, V. & Oks, E. Nonexistence of a local suppression in the ionization of hydrogen atoms by a low- frequency laser field of arbitrary strength. *Can. J. Phys.* **89**, 849–855 (2011).
26. Keldysh, L. Ionization in field of a strong electromagnetic wave. *Sov. Phys. JETP* **20**, 1307 (1965).
27. Thai, A., Hemmer, M., Bates, P., Chalus, O. & Biegert, J. Sub-250-mrad, passively carrier-envelope-phase-stable mid-infrared OPCPA source at high repetition rate. *Opt. Lett.* **36**, 3918–3920 (2011).
28. Husimans, Y. *et al*. Time-resolved holography with photoelectrons. *Science* **331**, 61 (2011).
29. Hickstein, D. D. *et al*. Direct visualization of laser-driven electron multiple scattering and tunneling distance in strong-field ionization. *Phys. Rev. Lett.* **109**, 073004 (2012).
30. Rudenko, A. *et al*. Resonant structures in the low-energy electron continuum for single ionization of atoms in the tunnelling regime. *J. Phys. B-At. Mol. Opt. Phys.* **37**, L407–L413 (2004).
31. Liu, Y., Liu, X., Deng, Y., Wu, C. & Gong, Q. Low-energy photoelectron angular distributions of above-threshold ionization of atoms and molecules in strong laser fields. *IEEE J. Sel. Top. Quant. Elec.* **18**, 195–200 (2012).
32. Dimitriou, K., Arbo, D., Yoshida, S., Persson, E. & Burgdorfer, J. Origin of the double-peak structure in the momentum distribution of ionization of hydrogen atoms driven by strong laser fields. *Phys. Rev. A* **70**, 061401 (2004).
33. Rudenko, A. *et al*. Coulomb singularity in the transverse momentum distribution for strong-field single ionization. *J. Phys. B-At. Mol. Opt.* **38**, L191–L198 (2005).
34. Pfeiffer, A. *et al*. Probing the longitudinal momentum spread of the electron wave packet at the tunnel exit. *Phys. Rev. Lett.* **109**, 83002 (2012).
35. Chalus, O., Thai, A., Bates, P. & Biegert, J. Six-cycle mid-infrared source with 3.8 μJ at 100 kHz. *Opt. Lett.* **35**, 3204–3206 (2010).

Acknowledgments

We acknowledge support from the Spanish Ministerio De Economia Y Competitividad (MINECO) through its Consolider Program (SAUUL-CSD 2007-00013), "Plan Nacional" (FIS2011-30465-C02-01) and the Catalan Agencia de Gestió d'Ajuts Universitaris i de Recerça (AGAUR) with SGR 2009-2013. This research has been partially supported by Fundació Cellex Barcelona, LASERLAB-EUROPE grant agreement 228334 and COST Action MP1203. J.D. was partially supported by FONCICYT Project 94142.

Author contributions

The experiments were designed by J.D., J.U., R.H. and J.B.; the REMI was commissioned by J.D., N.C., C.D.S., A.S. and J.B.; the light source was designed by J.B. and operated by M.H., M.B. and A.T.; the data was analyzed and interpreted by J.D., N.C., A.S., A.B., J.U., R.M. and J.B. Technical and vacuum support was given C.D.S. All authors discussed results and implications. J.D. and J.B. wrote the manuscript. All authors commented on the manuscript.

Additional information

Supplementary information accompanies this paper at http://www.nature.com/scientificreports

Competing financial interests: The authors declare no competing financial interests.

How to cite this article: Dura, J. *et al*. Ionization with low-frequency fields in the tunneling regime. *Sci. Rep.* **3**, 2675; DOI:10.1038/srep02675 (2013).